Photometric survey of stellar clusters in the outer part of M33. II. Analysis of HST/ACS images

K. Zloczewski and J. Kaluzny

Nicolaus Copernicus Astronomical Center,
ul. Bartycka 18, 00-716 Warsaw, Poland
e-mail: (kzlocz,jka)@camk.edu.pl

ABSTRACT

We have used deep ACS/WFC images of M33 to check nature of extended objects detected by the ground based survey of Zloczewski et al. (2008). A total of 24 candidates turned out to be genuine compact stellar clusters. In addition we detected 91 new clusters. Equatorial coordinates, integrated magnitudes and angular sizes are listed for all 115 objects. Fourty-two clusters have sufficiently red colors to be candidates for old globulars. For four clusters we extracted resolved stellar photometry. Object 33-3-018 located in the outer disk of M33 turned out to be a young cluster with an age estimated at 200-350 Myr. Cluster ZK-90 has an age of 3-5 Gyr. The remaining two clusters have intermediate ages ranging from one to a few Gyr.

catalogs– galaxies: individual (M33) – galaxies: star clusters

1 Introduction

Several surveys have been made to catalog stellar clusters in M33. In the last decade most of the clusters were found in the central part of the galaxy using imaging instruments on board of the Hubble Space Telescope (Chandar et al. 1999, 2001, Bedin et al. 2005, Park and Lee 2007). Wide-field searches for M33 clusters were also performed using ground-based observations (Hintler 1960; Melnick and D'Odorico 1978; Christian and Schommer 1982; Mochejska et al. 1998; Zloczewski et al. 2008, hereafter ZKH). The number of confirmed and candidate clusters is growing. Their on-line catalog is provided by Sarajedini and Mancone (2007, hereafter SM). These authors point out that the available sample is spatially incomplete. Indeed, only the central region of the galaxy with a size of about 15 $\times$ 15 arcmin^2 was surveyed systematically based on the HST WFPC2 images (see Fig. 1 of Park and Lee 2007). It is also worth to note that the faintest known M33 globular cluster candidates have $V \approx 21$ mag which corresponds to $M_V \approx -4$ (SM; ZKH). This can be compared with $M_V \approx -1$ observed for the faintest of the known globulars in the Milky Way (Koposov et al. 2007). One may expect that several faint globular clusters from M33 still await detection.

During the last two years several HST/ACS images covering various locations in the M33 have become publicly available. This prompted us to examine in detail some of candidate clusters included in our catalog of extended objects from the outer part of the galaxy (ZKH). Results of this examination are presented in Section 2. As it turned out, the analyzed images contain a few dozen of newly detected stellar clusters as well as several previously unconfirmed cluster candidates. Their catalog as well as integrated photometry are presented in Section 3. Section 4 is devoted to presentation and brief discussion of the color-magnitude diagrams (CMD) for 4 selected clusters. Summary and conclusions are given in Section 5.

2 Examination of ZKH cluster candidates

.

In our recent paper (ZKH) we presented a large sample of new candidate stellar clusters from the outer part of M33. An area of 0.75 deg^2 was surveyed based on deep $g'r'i'$ images collected with the CFHT telescope. The images had a subarcsecond seeing and a scale of 0.185 arcsec/pixel. Our catalog included 122 new likely compact stellar clusters, 3462 unclassified objects and 1155 galaxies. In addition, we recovered 41 clusters listed as "confirmed" in the SM catalog. Unclassified objects were selected in such a way that they could be considered candidates for unresolved stellar clusters.

Using HLA* archive we have identified and imported images of seven M33 fields observed with the ACS/WFC. These particular fields overlap (6 totally and 1 partially) with the region surveyed in ZKH. All images were obtained in the WFC mode with the 0.05 arcsec/pixel scale. The used filters include F475W, F606W and F814W. The frames were collected within programs #10190 (PI Garnett), #9480 (PI Rhodes) and #9837 (PI Ferguson). We note that these programs yielded also data for 7 fields located in the central part of M33. These fields were not covered by ZKH survey (one of ACS fields covering outskirts of M33 is also located out of ZKH survey area).

The examined ACS fields included 84 candidate clusters (unclassified objects) and 11 likely clusters from ZKH. Out of 84 candidate clusters 64 turned out to be background galaxies and 4 still cannot be classified with confidence. The remaining 16 candidates turned out to be genuine stellar clusters. As far as 11 likely clusters from ZKH are considered, we confirmed the classification for 8 of them. Among the remaining three objects two turned out to be galaxies and the nature of one remains unclear. In Table 1 we provide new classifications for all 95 extended ZKH sources identified on the ACS images. Object name from the ZKH catalog is listed in the first column of Table 1. Second column gives the name of the ACS/WFC image on which a given object can be seen. Object types assigned in columns 3 and 4 follow the convention adopted in the ZKH catalog.

3 Newly identified clusters

While checking the status of objects listed by ZKH we noted that the examined images contain some previously uncatalogued stellar clusters. Using images of all 15 fields observed within the programs listed in Sec. 2 we identified a total of 91 new stellar clusters. In addition, we were able to confirm cluster nature of one object (SM 57 = ZKH 33-3-021) which is not included on the list of "high confidence clusters" in the SM catalog. Positions and integrated photometry for these objects is provided in Table 2. The first 24 entries correspond to clusters from the ZKH list. The photometry is on the VEGAMAG system defined in Sirianni et al. (2005). The aperture magnitudes were extracted using Daophot code (Stetson 1987). The same aperture radius was used for all filters while extracting photometry for a given cluster. In Table 2 cluster IDs are followed by their equatorial coordinates. Column 4 provides the name of a data set on which a given object

*http://hla.stsci.edu

can be located, while columns 5-7 give VEGAMAG magnitudes for 3 considered bands. The aperture radius used for extraction of integrated photometry is listed in column 8. Its value is equal to the estimated angular radius of a given cluster. Last column gives projected distance from the center of M33 ($RA = 23.46212$ deg, $DEC = +30.66028$ deg, J2000.0).

Figure 1 shows color-magnitude diagram and color-color diagram for the clusters from Table 2. Two colors were available for 19 clusters only. One may see that the measured colors span a rather wide ranges. As for the magnitudes, the presented sample includes some of the faintest stellar clusters identified so far in M33. We list a total of 36 objects with $V > 20$[†] of which 9 have $21 < V < 22.0$. The recent catalog of Park & Lee (2007) includes just 8 clusters with $20 < V < 21.0$ and none with $V > 21.0$. Population of globular clusters from the Milky Way includes only old objects with ages exceeding about 10 Gyr. In general they show rather red integrated colors. The blue edge of unreddened color distribution occurs at $B - V \approx 0.55$ and $V - I \approx 0.84$ (Park & Lee 2007; Chandar et al. 2001). After correcting for the foreground extinction of $E(B-V) = 0.05$ (Schlegel et al. 1998) these colors transform to $F475W - F606W = 0.64$ and $F606W - F814W = 0.63$. These limiting values are marked with dotted lines in Fig. 1. One may see that our sample includes about 42 clusters from M33 with colors falling into the range observed for the Galactic globular clusters.

4 Analysis of selected clusters

Four clusters from Table 2 were chosen for a more detailed analysis. We focused our attention on low surface density objects located in the outer part of the galaxy. Their F814W filter images are presented in Fig. 2. Stellar profile photometry was extracted from individual FLT images using DOLPHOT package (Dolphin, 2000). In each case reductions were limited to the field of a size 800×800 pixel^2 (40×40 arcsec^2) field. If possible, these sub-frames were centered on the analyzed cluster. We followed the procedure described in DOLPHOT manual. A predetermined list of stellar positions was prepared by running DAOPHOT/ALLSTAR (Stetson, 1987) on deep drizzled image in the F814W band. Pixel area map correction and bad pixels maps were applied to FLT images. Revised HST/ACS zero-points[‡] were used to derive calibrated photometry on the VEGAMAG system for F475W, F606W and F814W bands.

In the following analysis we adopt for the foreground reddening $E(B-V) = 0.05$ (Schlegel 1998) for the M33 field. The corresponding extinction for ACS/WFC bands follows from relations given in Sirianni et al. (2005). As for the distance modulus, we adopt $(m - M)_0 = 24.64$ (Galleti et al. 2004).

4.1 Cluster ZK-90

With a projected angular distance from the galaxy center of $d = 38.0'$, the cluster ZK-90 is located in the far outskirts of M33. The only known cluster located at

[†] V magnitudes were estimated from F606W and F814W magnitudes using relations from Sirianni et al. 2005).

[‡] HST/ACS STScI webpage: http://www.stsci.edu/hst/acs/analysis/zeropoints

a larger galactocentric distance is M33-EC1 (Stonkute, 2008) with $d = 53'$. ZK-90 is also the faintest of all cataloged M33 stellar clusters. Its apparent magnitudes, obtained using calibrations from Sirianni et al. (2005) and photometry from Table 2 are $V = 20.90$ and $I = 19.80$. The unreddened integrated magnitude and color of the cluster can be estimated at $V_0 = 20.74$ and $(V-I)_0 = 1.00$. This implies an absolute magnitude $M_V = -3.90$.
Figure 3 shows the surface density profile of ZK-90 derived for stars with $F606W < 27.5$. No correction for the incompleteness of photometry was done. The cluster radius can be estimated conservatively at 2.2 arcsec, i.e. $\sim$10 pc. Panel (a) of Fig. 4 shows CMD for the 40×40 arcsec^2 field including the cluster. The prominent red giant clump (RC) is visible at $F606W = 25.05 \pm 0.16$ and $F606W - F814W = 0.74 \pm 0.05$. The subgiant branch can be easily traced down to $F606W \approx 27.5$, some 2.5 mag below the red clump. Stars forming these features belong to old or intermediate age populations (ages over 1 Gyrs). At the same time the brightest main sequence stars are observed at $F606W \approx 24.0$ which corresponds to an absolute magnitude $M_{\rm V} \approx -0.6$. Comparison with available stellar models shows that such bright and blue stars cannot be older than about 350 Myr. The CMD from Fig. 4a closely resembles CMD's for some other outer fields in M33 which were analyzed in detail by Barker et al. (2007).

The CMD for the region occupied by ZK-90 is shown if Fig. 4b (all stars are located at projected distance $d < 2.5$ arcsec from the cluster center). In Fig. 4c we show the diagram for the "comparison" field which is located close to ZK-90 and has the same area as the cluster field. Finally, Fig. 4d presents the cleaned CMD of the cluster from which the field interlopers were statistically removed. To obtain it, for each star from panel (c) the nearest counterpart was located in panel (b) and then removed. The cleaned CMD of the cluster shows 10-11 RC stars and 3 candidates for bright red giants. Subgiant branch and upper main sequence are rather poorly defined. Three isochrones plotted in Fig. 4d correspond to ages of 3, 4 and 5 Gyr (from left to right). They were extracted from Dartmouth Stellar Evolution Database (Dotter et al. 2008) for [Fe/H] $= -1.0$ and [α/Fe] $= 0.2$. Isochrones for [Fe/H] $= -0.5$ are too blue to match the observations. To transform model isochrones to the observational plane we adopted $E(F606W - F814W) = 0.05$ $A_{F606W} = 0.14$ (they follow from $E(B-V) = 0.05$ (Schlegel et al 1998)) and $(m-M)_0 = 24.64$ (Galleti et al. 2004). It may be concluded that the ZK-90 has an age between 3 and 5 Gyrs and its metallicity is close to [Fe/H] $= -1.0$.

A more detailed analysis of the cluster CMD is hampered by several difficulties. First of all, photometry of main-sequence stars is severely incomplete in the cluster field due to increased crowding. Moreover, comparisons of panels b and c of Fig. 4 shows that field stars significantly contaminate the cluster region. We note that ZK-90 contains about 10 red clump giants. It is therefore richer than well studied old open clusters from the solar vicinity like M67, NGC 188, NGC 2243 or Berkeley 39 (see CMD's in Carraro et al. (1994)).

4.2 Cluster 33-4-018

The cluster 33-4-018 is located at a projected distance of 27.1 arcmin from the center of M33. It is visible against the faint outer spiral arm labeled as IV by Sandage & Humpherys (1980). It was included in the catalog of planetary nebula candidates

(Magrini et al. 2001; object ID=11) based on the presence of Hα and OIII emission. On the composed color image HST_10190_46_ACS_WFC_F814W_F475W from the HST Legacy Archive the object appears as a resolved stellar cluster hosting several bright blue stars. Upper panels of Fig. 5 show CMDs for the 40×40 arcsec^2 field centered on the cluster. Stars marked with large symbols are located at a distance $r < 2.0$ arcsec from the cluster center. The bottom panel of Fig. 5 shows CMD for a nearby "comparison" field having the same area as the considered cluster region with $r < 2.0$ arcsec.

It is evident that the cluster region shows an excess of bright stars with $F606W < 24.5$ relatively to the comparison field. These stars are located on the upper main sequence as well as among bright red giants. The field population contains some main sequence stars as bright as $F606W \approx 22.5$ or $M_{\rm V} \approx -2.3$. However, as can be seen in Figs. 5cd, bright main sequence stars with $F606W < 24.5$ or $M_{\rm V} < -0.3$ are generally rare in this part of M33. One may also notice in Figs. 5ab that the completeness of cluster photometry diminishes rapidly for $F606W > 24.5$. This is due to crowding effect, which makes the detection of fainter stars in a region filled with brighter objects practically impossible. Figure 6 presents CMD of the cluster cleaned the same way as before from the field interlopers. An apparent lack of stars with $F606W < 26.5$ is entirely due to the incompleteness effect resulting in an "over-subtraction" of field stars from the cluster CMD.
We have attempted to estimate the age of the cluster by fitting model isochrones from Dotter et al. (2008). Since there is no spectroscopic information about the metallicity of 33-4-018, we considered models with three values of [Fe/H]: 0.0, -0.5 and -1.0. The isochrones for ages of 255, 300, 350 and 400 Myr are plotted in Fig. 6 along with the CMDs of the cluster. We adopted $E(B-V) = 0.05$ and $(m-M)_0 = 24.64$ while transforming the isochrones to the observational plane. One can see that none of age/metallicity combinations provides good fit to the observations. In general, all isochrones are too blue to reproduce location of cluster upper main sequence in F606W/F475W-F606W plane. This may be due to an intergalactic reddening which was not taken into account. However, even with assumed $E(B-V) = 0.05$ the solar metallicity models fail to reproduce location of cluster red giants. If we neglect the possible intergalactic reddening, the most acceptable fit is obtained for [Fe/H] $= -0.5$ and an age of 300-350 Myr. Assuming a total reddening of $E(B-V) \approx 0.12$ one may obtain reasonable fits to observed CMDs for [Fe/H] $= -0.5$ and [Fe/H] $= -1.0$. In such a case the preferred age would be 200-350 Myr.

In Fig. 5 one may see that CMDs of the analyzed 40×40 arcsec^2 field show a pronounced RC. There is no evidence for any noticeable blue horizontal branch, indicating the paucity of old and metal poor stars. Similar morphology of the CMD was observed by Barker et al. (2008) for 3 fields covering south-east outskirts of M33. The mean luminosity and color of the RC is correlated with average age and metallicity of the stellar population. The luminosity decreases with increasing age or metallicity, while the color becomes bluer with decreasing metallicity.

The deprojected distance of the 33-4-018 field from the center of M33 is 6.8 kpc. For RC stars from this field we have obtained average values of $<M_I> = -0.37$ and $<(V-I)_0> = 0.88$. This can be compared with results of Barker et al. (2008) for 3 other outer fields in M33 observed with ACS/WFC. For the field A1 located at deprojected distance of 9 kpc they measured $<M_I> = -0.41$ and $<(V-I)_0> = 0.94$,

while for the outermost field A3 at distance of 13 kpc they found $<M_I>=-0.38$ and $<(V-I)_0>=0.92$. If both sets of photometry are indeed on the same photometric system then one may conclude that old population stars in fields A3 and 33-4-018 have similar ages and metallicities. This is worth noticing, given that the deprojected galactocentric distances of both field differ by a factor of two.

4.3 Cluster SM-57

The object listed in the SM catalog under number 57 was first noticed by Christian & Schommer (1982). They included it on a list of unclassified non-stellar objects from M33 region. The SM catalog provides just its positional data along with a note that it is a possible galaxy. ZKH list the object under the name 33-3-021 and classify it as a possible cluster. Examination of ACS/WFC images shows that SM-57 is indeed a compact stellar cluster. It has an appearance resembling some presumed globular clusters from M33 (Sarajedini et al. 2000). SM-57 has absolute magnitude of $M_{\rm V}\approx-6.4$ ($V\approx18.4$) and half-light radius $r_h\approx3.7$ pc. This places it on the $M_{\rm V}/r_h$ diagram in the region occupied by several Milky Way globular clusters (van den Bergh 2008). However, as we show below, SM-57 is a rich intermediate age open cluster rather than an old globular cluster.

The object is visible against the spiral arm III of M33 (Sandage and Humphrey 1980). This makes stellar photometry in its field difficult, despite a relatively large angular distance of $d=17.6$ arcmin from the galaxy center. The upper panel of Fig. 7 shows the CMD for stars located in the ring $0.75<r<2.25$ arcsec centered on the cluster core. CMD's for nearby comparison field and surrounding 40×40 arcsec^2 field are shown in middle and bottom panels of Fig. 7, respectively. The CMD of the whole field exhibits a well populated red clump and an upper red giant branch. One may also notice a relatively large number of bright main-sequence stars with $F606W<23$ – see Figs. 4 & 5 for comparison. Apparently, the field hosts a noticeable population of young massive stars.

The available photometry allows only a very approximate estimation of cluster's age. A comparison of upper and middle panels of Fig. 7 shows that SM-57 has a well populated RC. The cluster seems to contain also some bright red giants with $F606W<24.0$. Such stars are missing from the CMD for the comparison field. We note that photometry in the comparison field extends about 1 mag deeper relatively to the ring covering the outer part of SM-57. This can be explained by increased crowding in the cluster area. Despite this effect, the cluster CMD shows an excess of stars at $F606W\approx26.0$ and $F606W-F814W\approx0.35$ (or $F475W-F606W\approx0.4$) relatively to the comparison field. These stars represent likely the top of clusters main sequence. In such a case the difference in luminosity between the RC and the main sequence top would be $\Delta F606W\approx\Delta V\approx1.0$. ΔV parameter is a robust age indicator for intermediate and old stellar clusters (Cannon 1970). Using calibration of Carraro & Chiosi (1994) we obtain for $\Delta V=1.0$ and assumed [Fe/H] $=-0.7$ an age of 1.0 Gyr. This estimate provides a rather safe lower limit on the cluster age. If the main-sequence of SM-57 were located below $F606W=26.0$, the cluster would be older than 1 Gyr. On the other hand, lack of clearly marked giant branch excludes an age exceeding 4-5 Gyr.

4.4 Cluster ZKH 33-6-012

Like the previous object, ZKH 33-6-012 is visible against the spiral arm III of M33. As can be seen in Fig. 2, it is located just on the edge of the field observed with ACS/WFC. The cluster is rather extended, with a total angular diameter exceeding 6.2 arcsec which corresponds to a linear diameter of 26 pc. In Fig. 8 we show CMD for stars detected inside radius $r = 3.1$ arcsec from the cluster center. The middle panel of this figure shows CDMs for the nearby comparison field having the same area as the cluster region. The CMD for 40×40 arcsec^2 region including the cluster is presented in the bottom panel. One may notice populous RC elongated in the reddening direction. Apparently this disk field suffers from substantial differential reddening. It is interesting that this effect operates even in a relatively small region occupied by the cluster (see the upper panel of Fig. 8).

The cleaned CMD of 33-6-012 is shown in Fig. 9. From this plot one may infer that the cluster possess about 60 RC giants. This estimate is in fact very conservative. There is no data for a significant part of the cluster, and no correction for incompleteness of photometry was applied. With no doubt 33-6-012 is a very rich cluster. Despite this, neither the cluster subgiant branch nor its main-sequence can be noticed in Fig. 9. Apparently the cluster turn-off is located below $F606W \approx 26.5$, i.e. more than 1 mag below the RC. This implies an age exceeding 1 Gyr. At the same time lack of noticeable subgiant branch and poorly populated AGB excludes ages over 4-5 Gyr. We conclude that 33-6-012 is a rich open cluster of intermediate age.

5 Discussion and conclusions

By examining archival ACS images of M33 galaxy we have confirmed cluster status for 24 candidates from ZKH catalog. Moreover, 91 new clusters were detected. Altogether these 115 clusters expand noticeably a sample of 215 "guaranteed" clusters included in the electronic edition of the SM catalog. The integrated $F606W - F814W$ color was obtained for 108 objects from our list. Fourt-two of these clusters have sufficiently red colors to be old globular clusters. However, one has to bear in mind that there is no unique relation between the integrated color and the age of a cluster. Figure 4 in Park & Lee (2007) shows clearly that on $M_V/B-V$ diagram there is a substantial overlap of regions occupied by open and globular clusters from the Milky Way. Hence, red color alone is not sufficient to declare that a given cluster from M33 has an age exceeding ~ 10 Gyr.

Eight out of 215 "guaranteed" clusters from the SM catalog have ages estimated at over 10 Gyr. Milky Way harbors about 150 globular clusters and it is about 6 times more luminous than M33. One could therefore expect, perhaps a bit naively, that M33 should possess about 25 old globular clusters. Our detection of 10 new candidates for old clusters confirms the conclusion of SM about a need for more complete and thorough survey of the whole M33 field. For the moment there are just 18 candidates for globular clusters in M33.

In fact, incompleteness of the sample of M33 clusters is not the only issue. The question about the actual age of the oldest M33 clusters is also far from being answered. Virtually all currently available age estimates are based on global parameters of a clusters like integrated colors and magnitudes (Chandar et al.

1999, 2001; Park & Lee 2007; SM) or integrated spectra (Morettii & Held 2006). Estimates relaying on integral photometry lead to identification of few clusters with age exceeding 10 Gyr. Moretti & Held (2006) used Lick indices measured from integrated spectra to derive age and metallicity for 42 clusters. They concluded that M33 globular clusters are relatively young with ages 8-9 Gyr. So far there are no old M33 clusters with resolved stellar photometry reaching the main sequence turnoff [§]. Sarajedini et al. (2000) obtained V/V-I diagrams for 10 halo clusters. Their photometry extends 2-2.5 mag below the horizontal branch level. This is still 1-1.5 mag above the level of the main sequence for old globulars. Moreover, available CMDs are heavily contaminated by field stars. For eight out of ten clusters studied by Sarajedini et al. (2000) it was possible to state that horizontal branch is located entirely redward of the RR Lyr instability strip. This points toward relatively young age and/or high metallicity. So far the only M33 cluster known to have a blue horizontal branch is M9 (Sarajedini et al. 1998; the case of C20 presented in that paper is in our opinion less convincing). This cluster has to be as old and metal-poor as some well studied globular clusters from the Milky Way. A presence of old and metal poor population in M33 is further supported by detection of RR Lyr stars in two outer regions of the galaxy (Sarajedini et al. 2006). However, actual fraction of old globulars and fraction of old stars in the M33 disk/halo remains unknown.

For two clusters analyzed in some detail in this paper we have succeeded with obtaining main-sequence photometry. Cluster ZK-90 turned out to have an intermediate age of 3-5 Gyr. Its photometry is exceptionally deep thanks to availability of long exposures and location in a relatively uncrowded region. Cluster 33-4-018, despite being located in the outer disk of M33, turned out to be quite young with an age of 200-350 Gyr. Such an age is not surprising, given that young bright and blue stars are observed in the disk of M33 at large galactocentric distances (Barker at al. 2007). Color-magnitude diagrams of the two remaining clusters show red clump stars and poorly populated giant branches. This points toward intermediate ages exceeding 1 Gyr.

We would like to point out that difficulty with obtaining main sequence photometry for old M33 clusters is due not only to crowding effects. Additional factor is a marginal sampling of the point spread function provided by ACS/WFC. This poor sampling makes very difficult the detection of fainter stars located in wings of brighter stars. The ACS/HRC mode offers pixel scale almost two times better compared to the WFC mode. This comes at expense of a slightly reduced quantum efficiency. Possibly, observations in the HRC mode of ACS would allow to obtain the first CMDs reaching down to the main-sequence for some old M33 clusters. Among obvious targets for such observation are M33-EC1 (Stonkute et al. 2008) and 34-5-022 from ZKH. These are two out of three outermost clusters known in M33. They are exceptionally extended and uncrowded, and are indeed ideal candidates for ACS/HRC observations.

Acknowledgements. We are greatful to Michael Barker for his comments on the orginal manuscript. Research of JK and KZ is supported by the Foundation for the Polish Science through grant MISTRZ. This paper is based on observations

[§] Two intermediate age open clusters with photometry reaching main-sequence turnoff are ZK90 (this paper) and C38 (Chandar et al. 2006)

made with the NASA/ESA Hubble Space Telescope, and obtained from the Hubble Legacy Archive, which is a collaboration between the Space Telescope Science Institute (STScI/NASA), the Space Telescope European Coordinating Facility (ST-ECF/ESA) and the Canadian Astronomy Data Centre (CADC/NRC/CSA).

REFERENCES

Barker, M. K., Sarajedini, A., Geisler, D., Harding, P. & Schommer, R. 2007, *Astron. J.*, **133**, 1138.

Bedin, L. R., Piotto, G., Baume, G., Momany, Y., Carraro, G., Anderson, J., Messineo, M. & Ortolani, S 2005, *Astron. Astrophys.*, **444**, 831.

Cannon, R. D. 1970, *MNRAS*, **150**, 111.

Carraro, G. & Chiosi, C. 1994, *Astron. Astrophys.*, **287**, 761.

Carraro, G., Chiosi, C., Bressan, A. & Bertelli, G. 1994, *Astron. Astrophys. Suppl. Ser.*, **103**, 375.

Chandar, R., Bianchi, L. & Ford, H. C. 1999, *Astrophys. J. Suppl. Ser.*, **122**, 431.

Chandar, R., Bianchi, L. & Ford, H. C. 1999, *Astrophys. J.*, **517**, 668.

Chandar, R., Bianchi, L. & Ford, H. C. 2001, *Astron. Astrophys.*, **366**, 498.

Chandar, R., Puzia, T. H., Sarajedini, A. & Goudfrooij, P. 2006, *Astrophys. J. Letters*, **646**, L107.

Christian, C. A., & Schommer, R. A. 1982, *Astrophys. J. Suppl. Ser.*, **49**, 405.

Dolphin, A. 2000, *P.A.S.P.*, **112**, 1383.

Dotter, A., Chaboyer, B., Jevremovic, D., Kostov, V., Baron, E.,& Ferguson, J. W. 2008, *Astrophys. J. Suppl. Ser.*, **178**, 89.

Galleti, S., Bellazzini, M. & Ferraro, F. R. 2004, *Astron. Astrophys.*, **423**, 925.

Hiltner, W. A. 1960, *Astrophys. J.*, **131**, 163.

Koposov, S. *et al.* 2007, *Astrophys. J.*, **669**, 337.

Magrini, L., Cardwell, A., Corradi, R.L.M., Mampaso, A. & Perinotto, M. 2001, *Astron. Astrophys.*, **367**, 498.

Melnick, J. & D'Odorico, S. 1978, *Astron. Astrophys. Suppl. Ser.*, **34**, 249.

Mochejska, B. J., Kaluzny, J., Krockenberger, M., Sasselov, D. D. & Stanek, K. Z. 1998, *Acta Astron.*, **48**, 455.

Moretti, A. & Held, E. V. 2007, *Stellar Populations as Building Blocks of Galaxies, Proceedings of IAU Symposium #241. eds. Vazdekis A. & Peletier R.F.*, **241**, 455.

Park, Won-Kee & Lee, Myung Gyoon 2007, *Astron. J.*, **134**, 2168.

Sandage, A. & Humphreys, R. M. 1980, *Astrophys. J.*, **236**, L1.

Sarajedini, A. & Mancone, C. L. 2007, *Astron. J.*, **134**, 447.

Schlegel, D. J., Finkbeiner, D. P. & Davis, M. 1998, *Astrophys. J.*, **500**, 525.

Sirianni, M. *et al.* 2005, *P.A.S.P.*, **117**, 1049.

Stetson, P. B. 1987, *PASP*, **99**, 191.

Stonkute, R. *et al.* 2008, *Astron. J.*, **135**, 1482.

van den Bergh, S. 2008, *MNRAS*, **390**, L51.

Zloczewski, K., Kaluzny, J. & Hartman, J. 2008, *Acta Astron.*, **58**, 23.

ZHK ID	name of HST set	ZHK type	HST type	ZHK ID	name of HST set	ZHK type	HST type
19-1-037	j8g803031	0	−1	25-1-010	j90o37011	0	−1
19-1-045	j8g803031	0	−1	25-1-011	j90o37011	0	−1
19-1-047	j8g803031	0	−1	25-1-013	j90o37011	0	−1
19-1-050	j8g803031	0	−1	25-1-015	j90o37011	0	−1
19-1-056	j8g803031	0	−1	32-5-017	j90o47011	0	−1
19-1-062	j8g803031	0	−1	32-5-018	j90o47011	0	−1
19-1-067	j8g803031	0	−1	32-5-021	j90o47011	0	−1
19-1-068	j8g803031	0	−1	32-5-022	j90o47011	0	−1
20-1-001	j8g802031	0	−1	32-5-024	j90o47011	0	1
20-1-006	j8g802031	0	−1	33-2-001	j90o47011	0	0
20-1-007	j8g802031	0	−1	33-2-003	j90o47011	0	1
20-1-008	j8g802031	0	−1	33-2-005	j90o47011	0	−1
20-1-012	j8g802031	0	−1	33-2-006	j90o47011	0	1
20-1-014	j8g802031	0	−1	33-2-007	j90o47011	0	−1
20-1-016	j8g802031	0	−1	33-2-010	j90o47011	0	1
20-1-017	j8g802031	0	−1	33-3-003	j90o47zbq	0	−1
20-1-018	j8g802031	0	−1	33-3-009	j90o31011	1	−1
20-1-020	j8g802031	0	−1	33-3-013	j90o31011	0	−1
20-1-021	j8g802031	0	−1	33-3-019	j90o31011	1	0
20-1-022	j8g802031	0	−1	33-3-020	j90o31011	0	1
20-1-023	j8g802031	0	−1	33-3-021	j90o31011	1	1
20-1-024	j8g802031	0	−1	33-4-018	j90o41011	1	1
20-1-025	j8g802031	0	−1	33-5-011	j90o41011	0	1
20-1-026	j8g801031	0	−1	33-5-013	j90o41011	0	1
20-1-027	j8g802031	0	−1	33-5-014	j90o41011	0	1
20-1-031	j8g801031	0	−1	33-5-015	j90o41011	0	1
20-4-002	j8g801031	0	−1	33-5-019	j90o41011	0	1
20-4-003	j8g801031	0	−1	33-5-020	j90o41011	0	0
20-4-007	j8g801031	0	−1	33-5-021	j90o41011	0	−1
20-4-008	j8g801031	0	−1	33-5-022	j90o41011	0	1
20-4-011	j8g801031	0	−1	33-5-023	j90o41011	0	−1
20-4-015	j8g801031	0	−1	33-6-002	j90o31011	0	−1
20-4-017	j8g801031	0	−1	33-6-003	j90o31011	0	−1
20-4-019	j8g801031	0	−1	33-6-005	j90o31011	0	−1
20-4-020	j8g801031	0	−1	33-6-007	j90o48a9q	0	0
20-4-022	j8g801031	0	−1	33-6-008	j90o31011	0	1
20-4-024	j8g801031	0	−1	33-6-009	j90o31011	1	1
20-4-027	j8g801031	0	−1	33-6-010	j90o31011	0	1
20-4-028	j8g801031	0	−1	33-6-012	j90o31011	1	1
20-5-021	j8g801031	0	−1	33-6-014	j90o31011	1	1
25-1-001	j90o37011	0	1	33-6-016	j90o48030	1	−1
25-1-002	j90o37011	0	−1	33-6-017	j90o48030	1	1
25-1-003	j90o37011	0	1	33-6-019	j90o31050	1	1
25-1-004	j90o37011	0	−1	33-6-020	j90o48a9q	0	0
25-1-005	j90o37011	0	−1	34-1-002	j90o41011	0	−1
25-1-007	j90o37011	0	−1	34-1-004	j90o41011	0	−1
25-1-008	j90o37011	0	1	34-2-001	j90o41011	1	1
25-1-009	j90o37011	0	−1				

Table 1: New classification of 95 objects from the ZKH catalog. Object types listed in columns 3/7 and 4/8 have the following meaning: -1 galaxy, 0 unclassified, 1 probable cluster. Objects with HST type set to 1 can be considered certain clusters. The data are available in electronic form at http://case.camk.edu.pl/results/index.html.

ID	$\alpha_{2000.0}[^\circ]$	$\delta_{2000.0}[^\circ]$	HST dataset	F475W	F606W	F814W	ap [″]	d [′]
25-1-008	23.24984	30.45544	j90o37011	–	20.51	19.50	1.00	16.5
25-1-003	23.26001	30.44884	j90o37011	–	20.41	20.09	1.15	16.4
25-1-001	23.26241	30.44294	j90o37011	–	20.16	19.60	1.00	16.6
34-2-001	23.26375	30.26727	j90o41011	20.70	20.27	19.69	2.15	25.7
33-4-018	23.27343	30.23981	j90o41011	19.61	19.19	18.68	2.75	27.1
33-6-019	23.28187	30.32722	j90o31050	–	–	–	–	22.0
33-6-017	23.28519	30.39167	j90o48030	–	20.03	19.48	1.50	18.5
33-5-022	23.28724	30.28100	j90o41011	21.92	21.34	20.73	0.80	24.5
33-5-019	23.29325	30.26272	j90o41011	21.86	21.16	20.37	1.05	25.4
33-6-014	23.30086	30.37688	j90o31011	20.59	19.84	18.94	1.50	18.9
33-6-012	23.30160	30.36632	j90o31011	20.22	19.57	18.80	2.00	19.5
33-6-010	23.30420	30.38527	j90o31011	19.37	19.40	19.47	0.80	18.4
33-5-015	23.30471	30.26116	j90o41011	21.86	21.45	21.06	1.20	25.3
33-5-014	23.30814	30.24217	j90o41011	20.96	20.30	19.64	1.75	26.3
33-5-013	23.30848	30.25453	j90o41011	20.84	20.50	20.04	1.50	25.6
33-6-009	23.31157	30.38852	j90o31011	19.83	19.23	18.54	2.00	18.1
33-5-011	23.31179	30.24392	j90o41011	20.72	20.40	20.09	1.65	26.2
33-6-008	23.31341	30.35390	j90o31011	19.68	19.57	19.46	1.75	19.9
33-3-021	23.33005	30.38955	j90o31011	19.01	18.23	17.58	2.00	17.6
33-3-020	23.33879	30.34219	j90o31011	18.59	18.36	18.06	1.50	20.1
33-2-010	23.35720	30.30032	j90o47011	–	20.56	20.51	1.00	22.3
33-2-006	23.37443	30.30926	j90o47011	–	19.83	19.64	1.15	21.5
33-2-003	23.38699	30.26299	j90o47011	–	20.23	20.04	1.10	24.2
32-5-024	23.40152	30.25905	j90o47011	–	21.57	21.20	0.75	24.3
ZK-1	23.27445	30.48041	j90o37011	–	19.71	19.35	1.20	14.5
ZK-2	23.28861	30.43520	j90o37011	–	19.91	19.46	1.10	16.2
ZK-3	23.29808	30.26763	j90o41011	21.37	21.22	21.01	1.25	25.0
ZK-4	23.29927	30.43011	j90o37011	–	20.48	20.01	1.00	16.2
ZK-5	23.30804	30.46668	j90o37011	–	19.41	18.82	1.50	14.1
ZK-6	23.32407	30.38805	j90o31011	22.12	21.50	20.79	0.80	17.8
ZK-7	23.33642	30.34723	j90o31011	21.77	21.31	20.79	0.85	19.9
ZK-8	23.33880	30.51694	j90o38030	–	20.06	19.28	0.75	10.7
ZK-9	23.34221	30.64115	j90o13011	–	19.07	18.24	1.70	6.3
ZK-10	23.34440	30.63339	j90o13011	–	20.61	19.84	0.75	6.3
ZK-11	23.34484	30.63883	j90o13011	–	19.62	18.81	1.00	6.2
ZK-12	23.34813	30.49819	j90o38030	–	20.90	20.31	0.75	11.4
ZK-13	23.34936	30.66017	j90o13011	–	18.95	18.46	1.65	5.8
ZK-14	23.35041	30.52869	j90o38030	–	19.90	19.24	1.20	9.8

Table 2: Properties of 115 stellar clusters from M33.

ID	$\alpha_{2000.0}[^\circ]$	$\delta_{2000.0}[^\circ]$	HST dataset	F475W	F606W	F814W	ap [″]	d [′]
ZK-15	23.35252	30.63051	j90o13011	–	19.24	18.58	1.45	5.9
ZK-16	23.35474	30.53838	j90o38030	–	20.47	19.72	1.10	9.2
ZK-17	23.35552	30.39420	j90o31011	21.38	20.96	20.52	0.90	16.9
ZK-18	23.35722	30.52218	j90o38030	–	20.47	19.98	0.85	9.9
ZK-19	23.35805	30.52263	j90o38030	–	20.29	19.36	1.00	9.9
ZK-20	23.36008	30.66655	j90o13011	–	19.62	18.90	0.75	5.3
ZK-21	23.36422	30.50099	j90o38030	–	19.57	18.70	1.00	10.8
ZK-22	23.36608	30.64695	j90o13011	–	19.38	18.84	1.20	5.0
ZK-23	23.37824	30.48730	j90o22011	–	18.57	18.08	0.90	11.2
ZK-24	23.38097	30.47834	j90o22011	–	18.55	17.87	1.40	11.7
ZK-25	23.38496	30.29347	j90o47011	–	21.22	20.60	0.95	22.4
ZK-26	23.38906	30.49606	j90o22011	–	19.69	19.54	0.90	10.6
ZK-27	23.39010	30.46933	j90o22011	–	18.35	18.11	1.30	12.0
ZK-28	23.39034	30.53376	j90o38030	–	18.64	18.58	1.50	8.4
ZK-29	23.39116	30.66503	j90o13011	–	18.85	18.36	1.25	3.7
ZK-30	23.39269	30.48331	j90o22011	–	20.03	19.02	1.35	11.2
ZK-31	23.39943	30.46234	j90o22011	–	20.68	20.45	0.70	12.3
ZK-32	23.40098	30.46576	j90o22011	–	19.40	18.76	1.40	12.1
ZK-33	23.40611	30.44973	j90o22011	–	20.34	19.99	0.75	13.0
ZK-34	23.40670	30.47824	j90o22011	–	20.88	20.36	1.00	11.3
ZK-35	23.40805	30.31439	j90o47011	–	20.14	19.65	1.25	20.9
ZK-36	23.41447	30.46871	j90o22011	–	20.05	19.01	1.00	11.8
ZK-37	23.41731	30.62925	j90o28050	–	18.31	17.74	1.25	3.0
ZK-38	23.41835	30.59441	j90o11011	–	–	–	–	4.6
ZK-39	23.41958	30.30716	j90o47011	–	20.84	20.62	1.25	21.3
ZK-40	23.42263	30.52041	j90o22011	–	18.45	18.28	1.35	8.6
ZK-41	23.42401	30.49234	j90o22011	–	19.15	18.67	0.75	10.3
ZK-42	23.42423	30.49280	j90o22011	–	19.87	19.75	0.75	10.2
ZK-43	23.42435	30.60058	j90o11011	–	18.76	18.21	1.05	4.1
ZK-44	23.42504	30.63887	j90o28050	–	18.65	17.95	1.25	2.3
ZK-45	23.42753	30.58304	j90o11011	–	19.91	19.02	1.00	5.0
ZK-46	23.42772	30.63930	j90o28050	–	18.74	18.20	1.00	2.2
ZK-47	23.42870	30.46291	j90o22011	–	20.12	19.73	1.00	12.0
ZK-48	23.42885	30.64173	j90o28050	–	19.04	18.58	0.80	2.0
ZK-49	23.43114	30.46896	j90o22011	–	19.59	18.89	1.00	11.6
ZK-50	23.43136	30.46618	j90o22011	–	–	–	–	11.8
ZK-51	23.43299	30.60363	j90o11011	–	19.69	19.13	0.75	3.7
ZK-52	23.43400	30.59037	j90o11011	–	19.16	18.48	1.20	4.4
ZK-53	23.43584	30.62600	j90o28050	–	19.20	18.69	1.00	2.5

Table 2: Continued.

ID	$\alpha_{2000.0}[^\circ]$	$\delta_{2000.0}[^\circ]$	HST dataset	F475W	F606W	F814W	ap [″]	d [′]
ZK-54	23.43603	30.60989	j90o11011	–	18.38	18.22	0.90	3.3
ZK-55	23.43675	30.57749	j90o11011	–	18.88	18.65	1.05	5.1
ZK-56	23.44052	30.58011	j90o11011	–	18.44	–	0.70	4.9
ZK-57	23.44390	30.57840	j90o11011	–	19.04	18.10	1.70	5.0
ZK-58	23.44463	30.60324	j90o11011	–	19.87	19.27	1.05	3.5
ZK-59	23.44480	30.59973	j90o11011	–	19.66	18.83	1.00	3.7
ZK-60	23.45235	30.61812	j90o11011	–	18.32	17.52	1.15	2.6
ZK-61	23.45237	30.58981	j90o11011	–	19.42	18.83	1.15	4.3
ZK-62	23.45638	30.47844	j90o22011	–	19.90	19.44	1.00	10.9
ZK-63	23.46244	30.59012	j90o11011	–	20.09	19.41	0.75	4.2
ZK-64	23.47172	30.59045	j90o11011	–	–	–	–	4.2
ZK-65	23.47211	30.52424	j90o27011	–	19.92	19.70	0.80	8.2
ZK-66	23.47246	30.58260	j90o11011	–	19.48	18.85	0.80	4.7
ZK-67	23.47381	30.53706	j90o27011	–	19.98	19.16	0.90	7.4
ZK-68	23.47563	30.60187	j90o11011	–	20.11	19.63	0.70	3.6
ZK-69	23.47662	30.53999	j90o27011	–	19.25	18.54	1.25	7.3
ZK-70	23.49103	30.53941	j90o27011	–	19.37	–	1.10	7.4
ZK-71	23.49758	30.53338	j90o27011	–	19.36	–	1.00	7.8
ZK-72	23.49809	30.60674	j90o11011	–	19.67	19.47	0.55	3.7
ZK-73	23.49878	30.53337	j90o27011	–	19.77	19.04	1.00	7.8
ZK-74	23.50726	30.56839	j90o27011	–	19.23	18.50	1.50	6.0
ZK-75	23.50785	30.57299	j90o27011	–	18.81	17.86	1.70	5.7
ZK-76	23.50936	30.54385	j90o27011	–	19.05	18.13	1.15	7.4
ZK-77	23.51365	30.46550	j90o14050	–	17.81	17.40	2.35	12.0
ZK-78	23.51431	30.56153	j90o27011	–	19.71	19.40	0.95	6.5
ZK-79	23.51929	30.45594	j90o14050	–	19.65	19.06	2.15	12.6
ZK-80	23.52071	30.47216	j90o14050	–	20.50	19.74	1.00	11.7
ZK-81	23.52800	30.46783	j90o14050	–	19.47	18.91	1.30	12.0
ZK-82	23.52839	30.56815	j90o27011	–	19.84	19.03	1.00	6.5
ZK-83	23.52988	30.56281	j90o27011	–	19.41	18.76	1.50	6.8
ZK-84	23.54026	30.41803	j90o14050	–	20.02	19.75	1.25	15.1
ZK-85	23.54544	30.47564	j90o14050	–	19.77	19.50	1.40	11.9
ZK-86	23.55380	30.47947	j90o14050	–	18.13	17.65	1.50	11.8
ZK-87	23.55629	30.47884	j90o14050	–	19.81	19.15	1.60	11.9
ZK-88	23.57400	30.45241	j90o14050	–	20.82	20.44	0.85	13.7
ZK-89	23.57770	30.45526	j90o14050	–	20.05	19.34	1.15	13.7
ZK-90	23.75930	31.23930	j8q802010	–	20.66	19.84	2.40	38.0
ZK-91	23.76993	31.19940	j8q802010	–	21.89	21.64	1.00	36.0

Table 2: Continued.

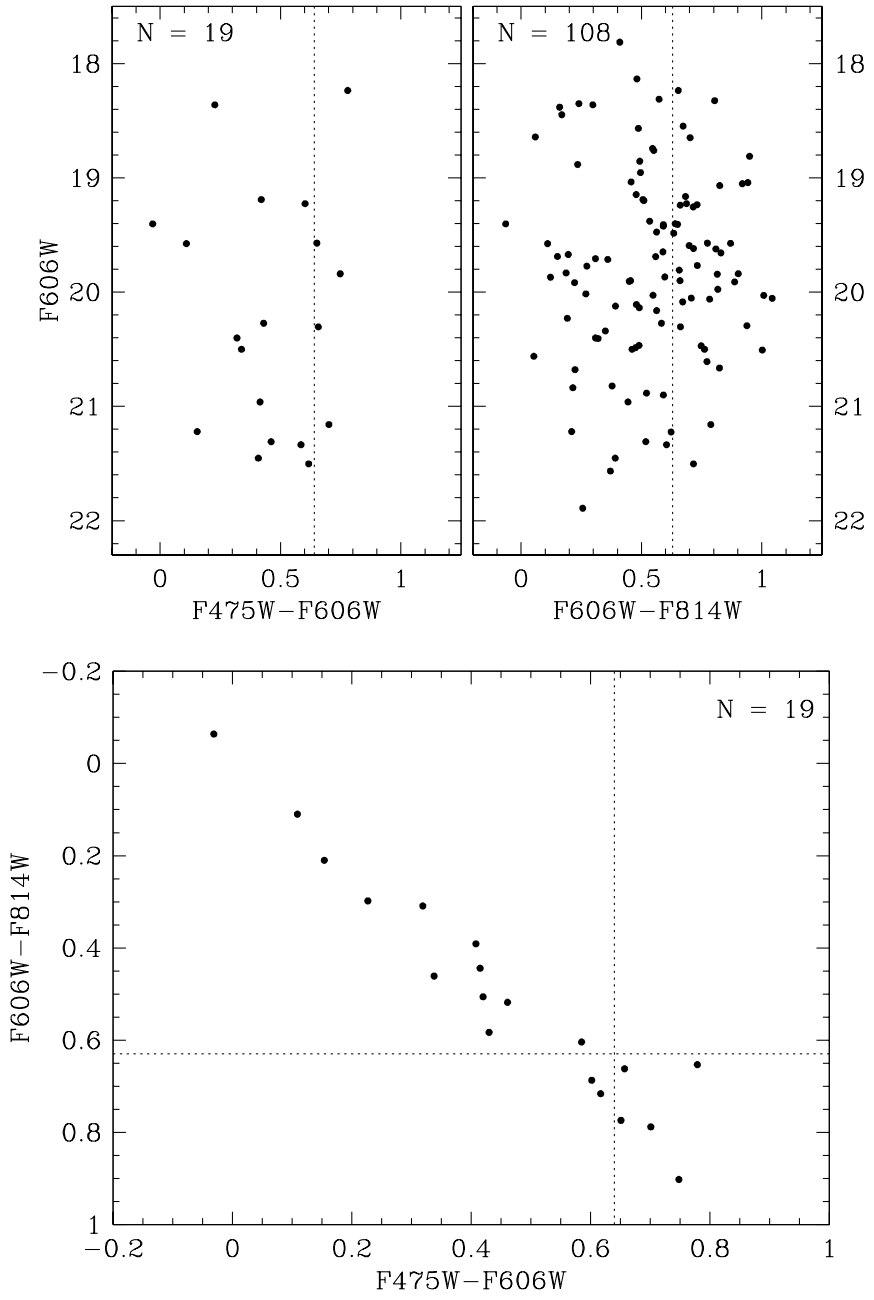

Figure 1: Color-magnitude and color-color diagrams for M33 clusters from Table 2. The dashed lines mark blue edges of color distribution for globular clusters from the Milky Way.

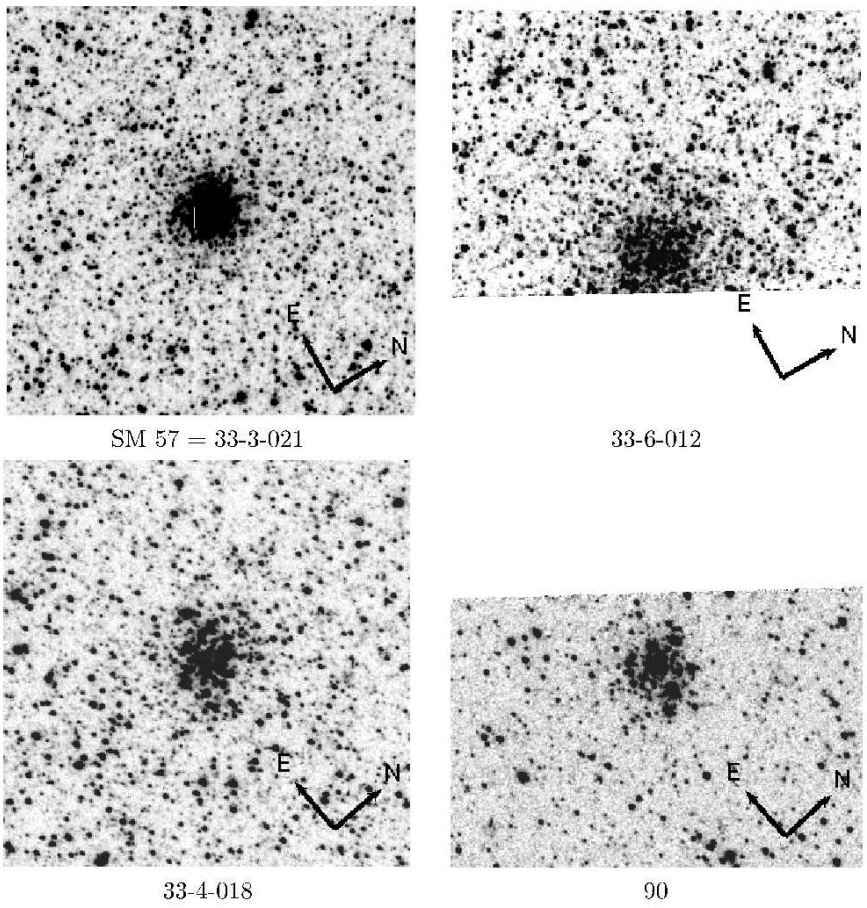

Figure 2: F814W images of clusters analyzed in Sec. 4. All charts are 16 arcsec wide.

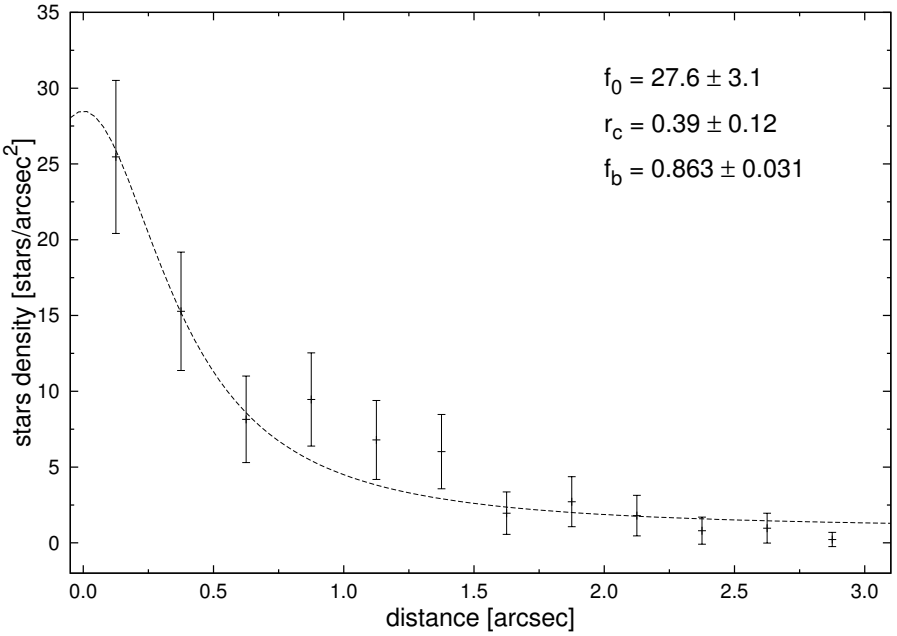

Figure 3: Surface density profile of ZK-90 for stars with F606W<27.5. King's profile fit is shown with the solid line.

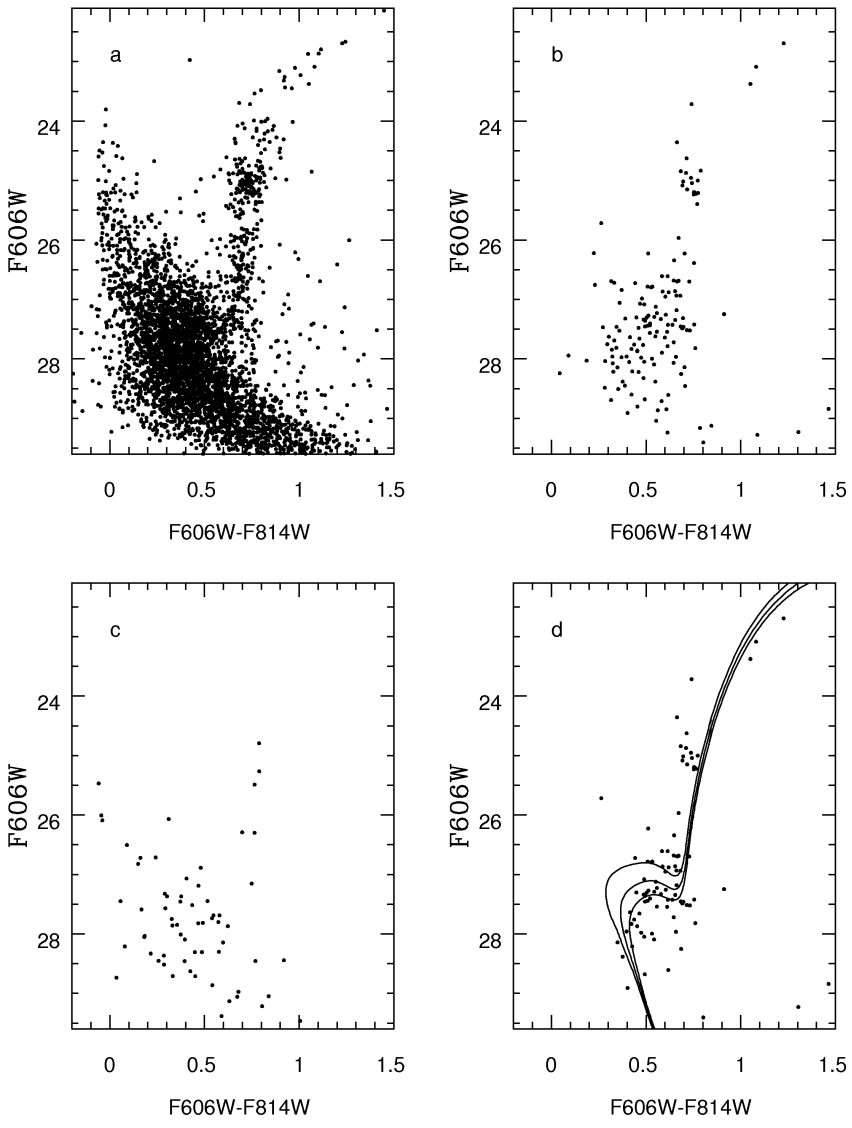

Figure 4: Color magnitude diagrams for the cluster ZK-90 and the surrounding field. See text for details.

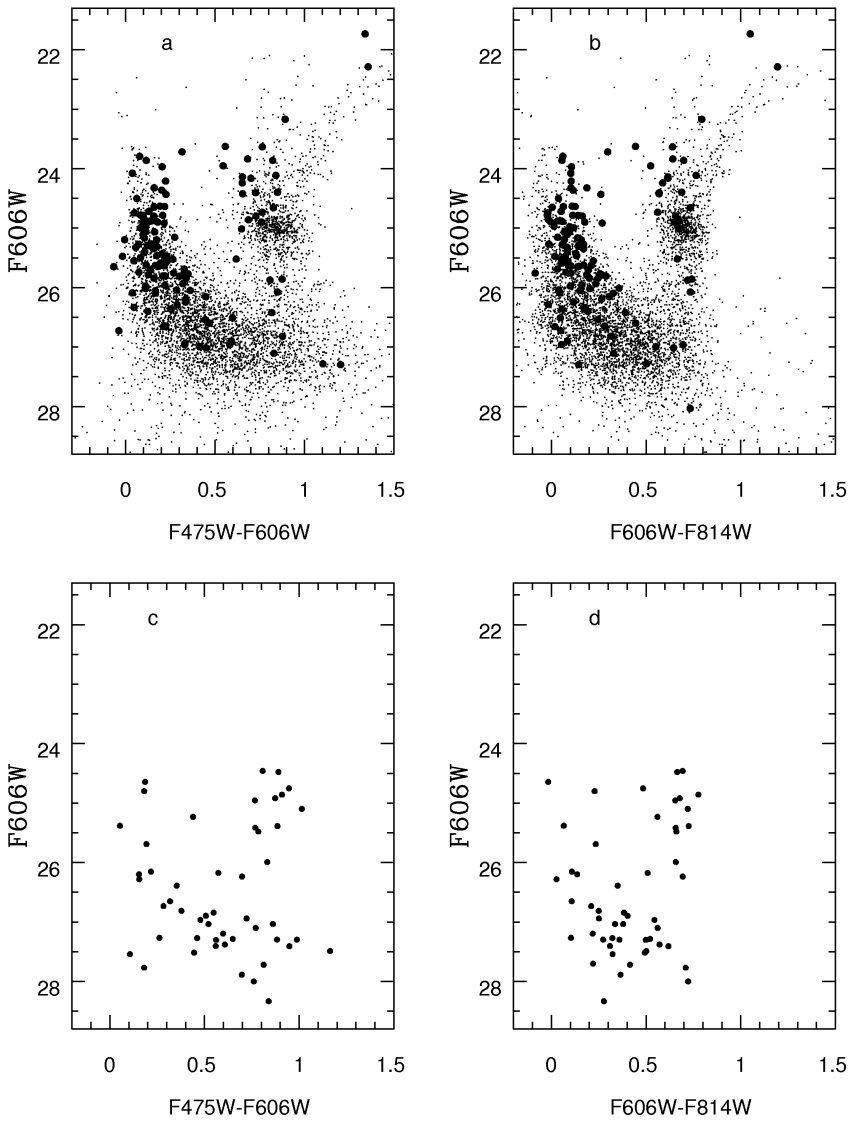

Figure 5: Upper panel: CMDs of the cluster 33-4-018 (filled circles) and the surrounding field (small dots). Lower panel: CMDs for the comparison field having the same area as the cluster field.

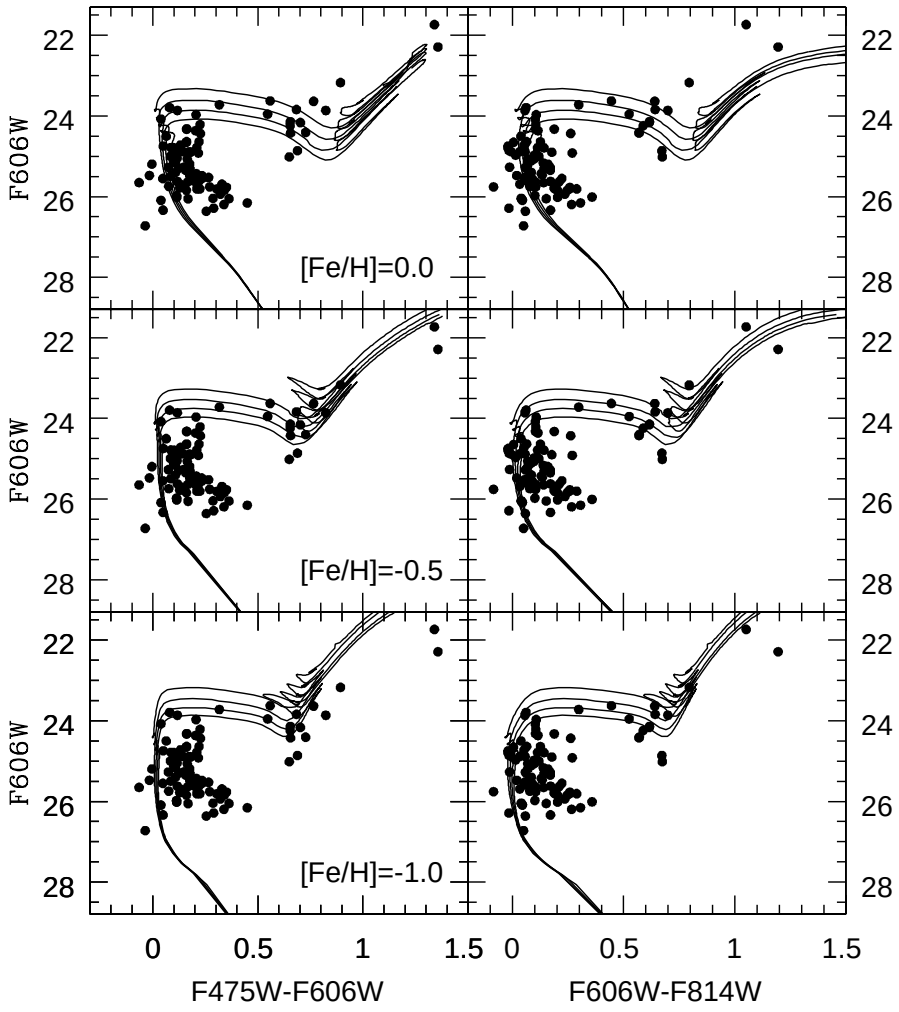

Figure 6: Field stars corrected CMDs of the cluster 33-4-018. Darthmouth isochrones for ages 250, 300, 350 and 400 Myr are marked with continuous lines. Top, middle and bottom panels show isochrones for [Fe/H]$=0.0$, [Fe/H]$=-0.5$ and [Fe/H]$=-1.0$, respectively.

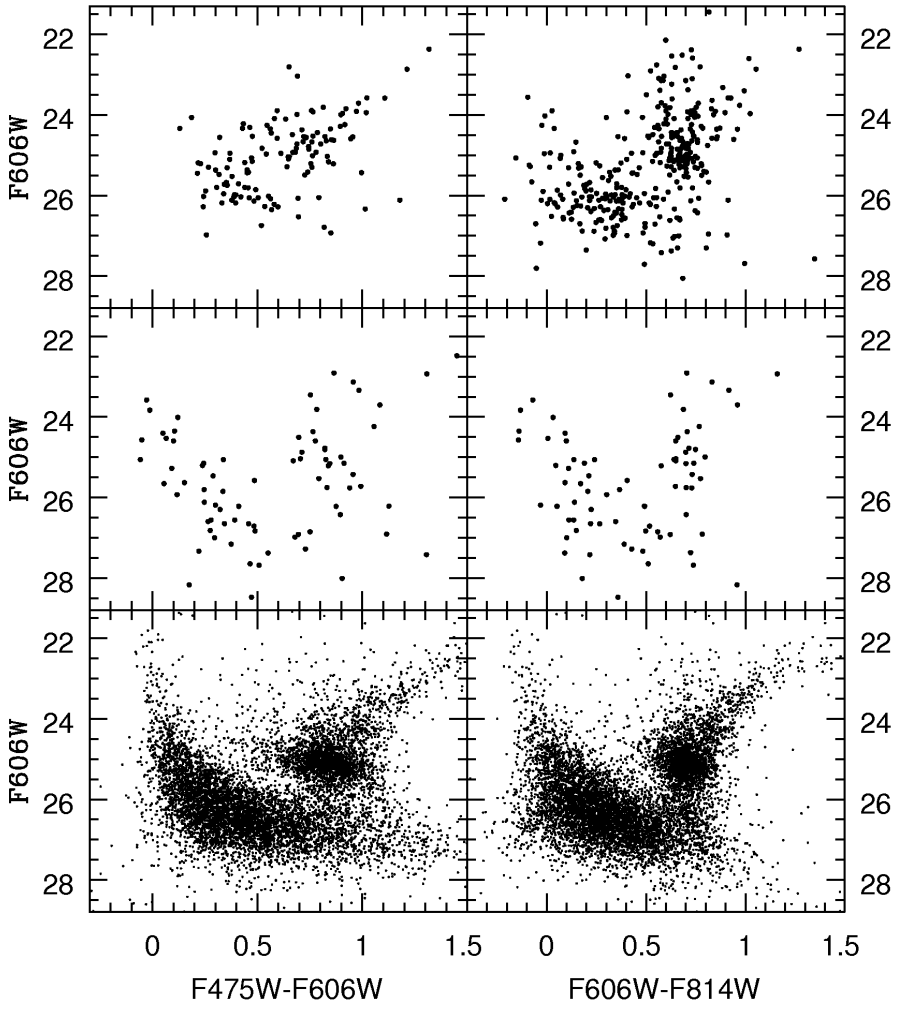

Figure 7: Color-magnitude diagrams for SM-57 (top), the nearby comparison field (middle) and 40×40 arcsec^2 region around the cluster (bottom). The comparison field has the same area as the cluster field.

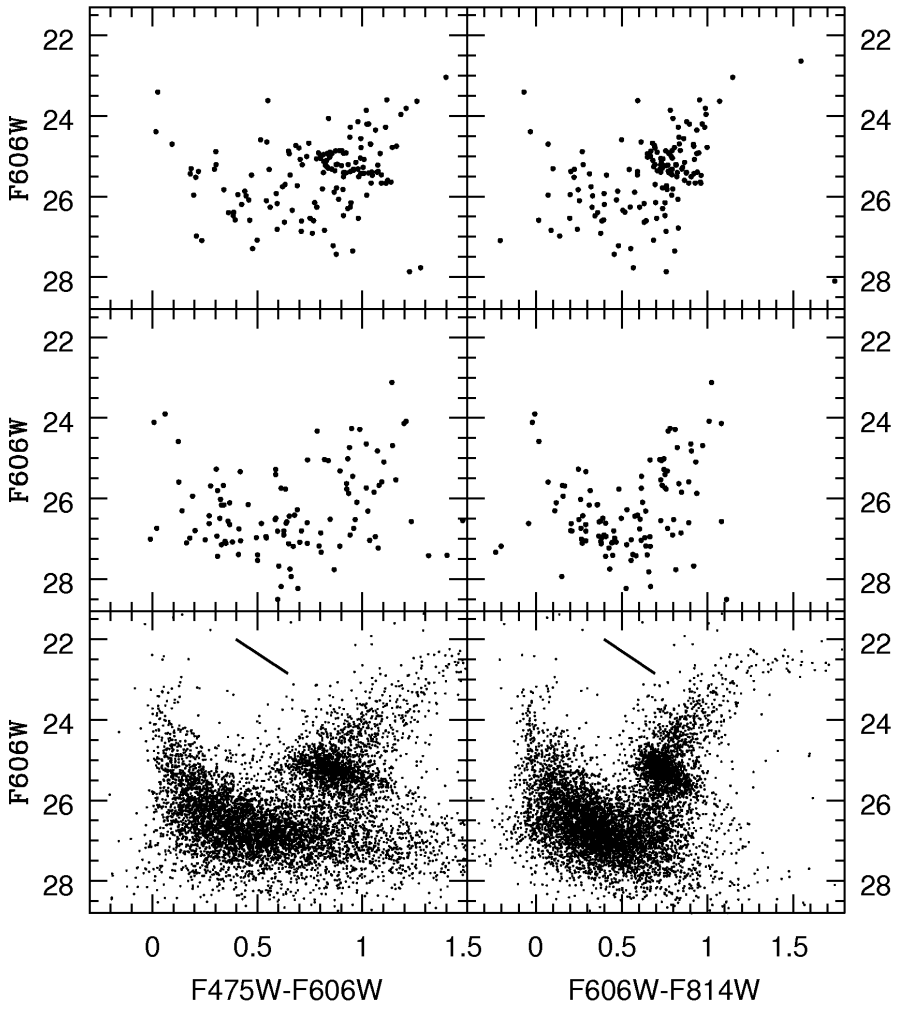

Figure 8: Color-magnitude diagrams for 33-6-012 (top), the nearby comparison field (middle) and 40×40 arcsec^2 region around the cluster (bottom). The reddening vector for $E(B-V) = 0.3$ is shown in the lower panel.

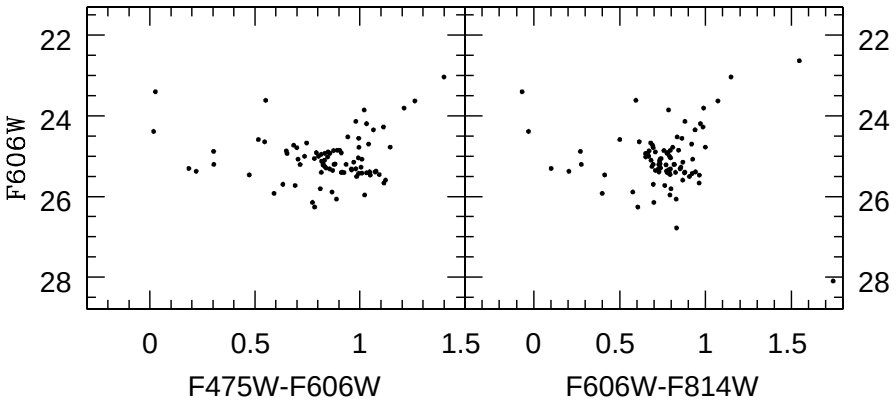

Figure 9: Cleaned CMDs of the cluster 33-6-012.